Tree Physiology 27, 1687–1699

Linking leaf and tree water use with an individual-tree model

BELINDA E. MEDLYN,[1–3] DAVID A. PEPPER,[1] ANTHONY P. O'GRADY[4] and HEATHER KEITH[5,6]

[1] *School of Biological, Earth and Environmental Sciences, University of NSW, Sydney 2052, Australia*

[2] *Present address: Department of Biological Sciences, Macquarie University, NSW 2109, Australia*

[3] *Corresponding author (bmedlyn@bio.mq.edu.au)*

[4] *School of Plant Science, University of Tasmania, Private Bag 55, Hobart 7001, Tasmania, Australia*

[5] *CSIRO Climate Program, P.O. Box 3023, Canberra, ACT 2601, Australia*

[6] *Present address: The Fenner School of Environment and Society College of Science, The Australian National University, Canberra, ACT 0200, Australia*

Received January 14, 2007; accepted May 2, 2007; published online September 4, 2007

Summary We tested the ability of a model to scale gas exchange from leaf level to whole-tree level by: (1) measuring leaf gas exchange in the canopy of 10 trees in a tall *Eucalyptus delegatensis* RT Baker forest in NSW, Australia; (2) monitoring sap flow of the same 10 trees during the measurement week; and (3) using an individual-tree-based model (MAESTRA) to link the two sets of measurements. Photosynthesis and stomatal conductance components of the model were parameterized with the leaf gas exchange data, and canopy structure was parameterized with crown heights, dimensions and leaf areas of each of the measurement trees and up to 45 neighboring trees. Transpiration of the measurement trees was predicted by the model and compared with sap flow data. Leaf gas exchange parameters were similar for all 10 trees, with the exception of two smaller trees that had relatively low stomatal conductances. We hypothesize that these trees may have experienced water stress as a result of competition from large neighboring trees.

The model performed well, and in most cases, was able to replicate the time course of tree transpiration. Maximum rates of transpiration were higher than measured rates for some trees and lower than measured rates for others, which may have been a result of inaccuracy in estimating tree leaf area. There was a small lag (about 15–30 minutes) between sap flow and modeled transpiration for some trees in the morning, likely associated with use of water stored in stems. The model also captured patterns of variation in sap flow among trees. Overall, the study confirms the ability of models to estimate forest canopy transpiration from leaf-level measurements.

Keywords: canopy modeling, Eucalyptus delegatensis, gas exchange, scaling, stomatal conductance, transpiration.

Introduction

Predictions of forest carbon and water balances are necessary to answer many scientific questions, such as the effects of forest management on carbon sequestration, groundwater recharge and climate (e.g., Walker et al. 2002, Lasch et al. 2005, Silva et al. 2006, Vano et al. 2006, White et al. 2006) and the impacts of global change on forest production and water use (e.g., Hatton et al. 1992, Gordon and Famiglietti 2004, Morales et al. 2005, Gedney et al. 2006). The models used to predict such impacts usually involve scaling of ecophysiological processes over a range of temporal and spatial scales (Jarvis 1995). In particular, scaling from leaf-level physiology to predict canopy responses, either explicitly or implicitly, lies at the heart of many models (Medlyn et al. 2003).

For predictions to be credible, it is necessary to verify or test the accuracy of the models that generate them, but there are significant challenges in performing meaningful tests (Mayer and Butler 1993, Oreskes et al. 1994, Rykiel 1996, Medlyn et al. 2005*a*). One challenge arises because data to test model output are often the outcome of a range of processes. Eddy covariance data, for example, include contributions from overstory, understory and soil processes, and soil water or catchment runoff data include processes such as interception, soil evaporation, evapotranspiration and soil drainage. Mismatches between model output and data can be difficult to understand, because any of the component processes could be at fault. Also, errors in the representation of one process may be compensated for by errors in another process.

In this study, we made use of closely related datasets to directly test the ability of a model to scale from leaves to tree canopies. Measurements of leaf gas exchange and tree sap flow were made concurrently and on the same trees. An individual-tree-based model (MAESTRA; Medlyn 2004) was used to scale from the leaf-level measurements to predict transpiration of the tree crowns. Predicted transpiration was then compared with measured sap flow. Because sap flow represents the loss of water from the tree crown, this exercise directly tests the parameterization of the leaf-level model and its ability to scale to the canopy.

Although sap flow measurements have been previously

used to test canopy models (e.g., Köstner et al. 1998, Williams et al. 2001, Meiresonne et al. 2003), the current work is novel in that (1) concurrent measurements of leaf-level and tree-level processes were made and (2) the model simulates radiation absorption by individual tree crowns, rather than by the stand as a whole. When sap flow measurements are used to test one-dimensional stand models, the measurements must be averaged across a number of representative trees to obtain stand-scale water use. By using an individual-tree model, we can avoid this averaging process and instead investigate the ability of the model to simulate features of sap flow of individual trees. The peak transpiration rate and diurnal pattern of sap flow vary among trees because of differences in tree size and aspect. We tested the ability of the model to capture these differences among trees.

The measurements were made in a tall *Eucalyptus delegatensis* RT Baker forest at the Tumbarumba eddy flux site (Leuning et al. 2005) on the western side of the Great Dividing Range in southern NSW, Australia. This forest is highly productive despite its relatively open canopy. It is typical of the cool temperate forests of southeastern Australia, which, because of their high productivity, are economically valuable and represent an important carbon sink. Eddy flux measurements at Tumbarumba estimate the net ecosystem exchange (NEE) of the forest to be about 650 g C m^{-2} $year^{-1}$ in a year of high rainfall, but it is dramatically reduced by drought (Leuning et al. 2005). Model simulations are being used together with measurements of carbon stocks and respiratory fluxes to develop a carbon budget for the forest and its response to drought (Keith et al., unpublished data).

Materials and methods

Site

The study site is located in the Bago State Forest near Tumbarumba in temperate south-eastern New South Wales, Australia. Elevation of the site is 1200 m, and long-term mean annual precipitation is 986 mm (Leuning et al. 2005). *Eucalyptus delegatensis* is the dominant species in this wet sclerophyll forest. The forest is tall but relatively open: mean tree height is about 40 m and leaf area index is about 1.4.

Measurements were made on 10 trees, two at each of five sub-sites located within 1 km of the Tumbarumba eddy flux tower (35°39′20.6″ S, 148°9′7.5″ E; Leuning et al. 2005). The height and diameter at breast height (DBH) of each measurement tree are given in Table 1. Measurements were made during May 6–10, 2002 (Southern Hemisphere autumn). Incident radiation and air temperature over these five days are shown in Figure 1. Soil water storage was monitored by time-domain reflectometry close to the eddy flux tower, and during this period, it was about 325 mm in the top 120 cm of soil. Sap flow was monitored on each tree throughout the week, and gas exchange measurements were made at a different sub-site each day. A 20-m-tall cherry picker mounted on a truck was used to access the forest canopy. At Sub-sites 1–4, we could reach only the bottom third of the tree crowns from the cherry picker, whereas at Sub-site 5, we were able to sample leaves from the top of the tree crowns (Table 1).

The canopy environment at each sub-site was characterized by measuring the dimensions of all large trees that would affect direct solar radiation reaching the canopy of the measurement trees. Diameter at breast height, tree height, height to crown base and crown diameter were recorded for each tree, as well as distance and bearing from the first measurement tree. Between 25 and 45 trees were measured at each sub-site. Mean DBH and height for each sub-site are given in Table 1, and maps of the data are shown in Figure 2. The approximate positions of the leaves monitored for gas exchange are indicated, showing that the aspect of the measured leaves varied among sub-sites.

Gas exchange measurements

Leaf gas exchange was measured with a Li-Cor LI-6400 portable Photosynthesis Measuring System (Li-Cor, Lincoln, NE) with attached light source (6400-02 LED). Two sets of measurements were taken. Spot measurements of photosynthesis and stomatal conductance were made in ambient light, measured with a hand-held PAR sensor, throughout the day. In addition, four leaves (two from each tree) were chosen each day

Table 1. Diameter at breast height (DBH), height and height to crown base of measured trees. Mean DBH, height and height to crown base of dominant trees at each sub-site are also given. Date indicates when the gas exchange measurements were made at the site.

Date	Sub-site	Tree	DBH (cm)	Height (m)	Crown base (m)	Mean DBH (cm)	Mean height (m)	Mean crown base (m)
May 9	1	1	45.1	34.9	20.3	62.8	34.9	20.8
		2	56.6	33.1	19.3			
May 6	2	3	32.1	29	18	63.1	38.2	23.5
		4	42.3	29.4	19			
May 8	3	5	53.2	37.3	16.8	60.9	37.1	21.2
		6	38.6	32.5	18.9			
May 7	4	7	63.1	30.7	18.1	55.8	32.3	19
		8	41.1	24.3	17			
May 10	5	9	30.4	23.7	14.9	69.2	39.4	23.7
		10	28.5	20.6	13.4			

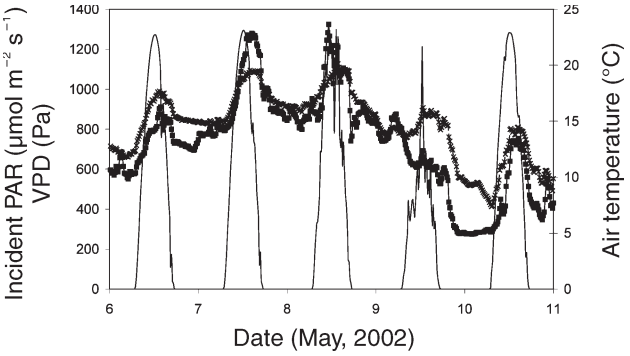

Figure 1. Meteorological data over the five days of measurement. Data were measured at the top of the eddy flux tower (70 m) and corrected to canopy height. Symbols: solid line = incident photosynthetically active radiation (PAR); closed squares = vapor pressure deficit (VPD); and crosses = air temperature.

for detailed measurements of photosynthetic response to CO_2 concentration and irradiance (A–C_i and A–PAR curves). These measurements were interspersed with the spot measurements. All measurements were made at ambient temperature and relative humidity.

Leaves for measurements were randomly selected, with equal numbers selected from each tree accessible from the cherry picker each day. Two leaf age classes were present and were equally represented in measurements. No differences between leaf classes could be statistically detected, so data from the two classes were combined for this analysis.

At the end of each day, all leaves used for gas exchange measurements were harvested by excising the twig to which the leaves were attached. Leaves were oven-dried at 60 °C for 24 h to constant mass and finely ground. A 0.1 g sample was analyzed for nitrogen and phosphorus by semi-micro Kjeldahl digestion and automated colorimetry (Technicon TRAACS 800; Rayment and Higginson 1992). A second sample was analyzed for chlorophyll a and b by extracting chlorophyll from the sample with dimethylformamide and then determining absorptance (Perkin Elmer UV/VIS Spectrometer Lambda 2) at 660.8 nm for chlorophyll a and 642.5 nm for chlorophyll b (Porra et al. 1989).

Variation in leaf properties through the canopy was also investigated. Additional leaves were harvested from each tree crown with an extendable pruner, classified according to canopy position (top, middle or bottom) and leaf age, and analyzed for leaf nitrogen and phosphorus as previously described.

Sap flow measurements

Sap flow was measured in each tree by the compensation heat pulse technique with commercially available sap flow loggers (Greenspan Technology, Warwick, QLD). Heat pulse velocity was measured at 15-min intervals at four depths in the sapwood. The solutions of Swanson and Whitfield (1981) were used to correct for the effects of wounding, assuming a wound width of 3.1 mm (O'Grady 2000). Heat pulse velocity was converted to sap velocity as described by Edwards and Warwick (1984), and sap velocity was scaled to tree water use by the weighted average technique of Hatton et al. (1990). Wood cores were taken from each tree for determination of sapwood depth and volume fractions of wood and water contents. Sapwood depth was distinguished from heartwood by a distinct colour change. Sap flow data for Tree 7 were omitted from the analyses because of obvious errors in the dataset.

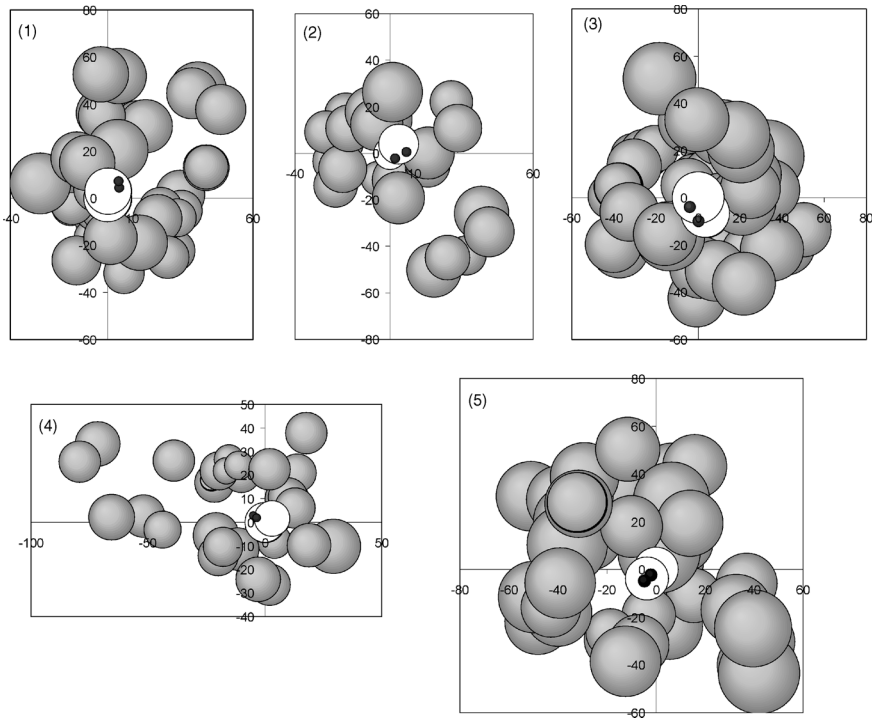

Figure 2. Maps of tree positions and crown dimensions for each sub-site. The measurement trees are shown in white. All trees whose crowns affected radiation incident on the measurement tree crowns are shown in gray. Black dots indicate the approximate location of leaf gas exchange measurements. At each site, the first measurement tree (i.e., Trees 1, 3, 5, 7 and 9) is located at (0,0). North is up.

Leaf model

Spot measurements of stomatal conductance (g_s; mol m^{-2} s^{-1}) were fitted to the Ball-Berry equation (Ball et al. 1987):

$$g_s = g_0 + g_1 \frac{A h_r}{C_a} \quad (1)$$

where A is assimilation rate (μmol m^{-2} s^{-1}), h_r is relative humidity, C_a is ambient CO_2 concentration (μmol mol^{-1}) and g_0 and g_1 are parameters. Two alternative leaf models were considered (Jarvis 1976, Leuning 1995) but Equation 1 resulted in the best fit to the data. This model of g_s assumes no effect of soil water supply.

To use Equation 1 in up-scaling, it is necessary to model leaf photosynthesis (A). Here, the Farquhar et al. (1980) model of leaf photosynthesis was fitted to the A–C_i and A–I response curves by nonlinear least squares regression to obtain the key photosynthetic parameters J_{max25}, the potential rate of electron transport at 25 °C (μmol m^{-2} s^{-1}), V_{cmax25}, the maximum rate of carboxylation by Rubisco at 25 °C (μmol m^{-2} s^{-1}), R_{d25}, the dark respiration rate at 25 °C (μmol m^{-2} s^{-1}), and α_J, the quantum yield of electron transport. The following assumptions were made when fitting the model. The light response of electron transport was assumed to be a non-rectangular hyperbola, with the curvature parameter Θ set to 0.7. Temperature dependences of the CO_2 compensation point, Γ^*, and the Michaelis-Menten constant for Rubisco, K_m, were taken from Bernacchi et al. (2001). Temperature dependences of J_{max} and V_{cmax} were taken from measurements made on *Eucalyptus pauciflora* Sieb. ex Spreng. by Kirschbaum and Farquhar (1984), as re-parameterized by Medlyn et al. (2002). These temperature dependences were confirmed by fitting the parameters at measurement temperature and checking the relationship with leaf temperature. Leaf R_d was estimated as

$$R_d = 0.41 e^{0.0575 T_a} \quad (2)$$

from nighttime leaf measurements, where T_a is air temperature.

Tree model

The MAESTRA model (Wang and Jarvis 1990, Medlyn 2004) was used to predict transpiration of the measurement trees throughout the study period. In this model, the forest canopy is represented as an array of tree crowns, whose positions and dimensions are specified. Radiation absorption, photosynthesis and transpiration are calculated for an individual "target" crown. The distribution of leaf area within the target crown is specified, as is the leaf angle distribution. The target crown is divided into 60 grid points, and the radiation penetrating to each grid point is calculated for three wavebands (PAR, near infrared and longwave). Direct, diffuse and scattered radiation are considered separately. The absorbed radiation at each grid point drives the photosynthesis and transpiration routines. Photosynthesis is calculated from the Farquhar et al. (1980) model. Stomatal conductance is calculated from Equation 1. Transpiration is calculated by applying the Penman-Monteith equation (see Appendix) at each gridpoint and summing over the gridpoints. This model has been widely applied and has been previously tested against radiation absorption (e.g., Wang and Jarvis 1990) and eddy flux data (e.g., Medlyn et al. 2005*b*). Further information about the MAESTRA model, together with a full bibliography for the model, can be obtained from the website www.bio.mq.edu.au/maestra/.

The model was parameterized with crown positions and dimensions for each sub-site (Figure 2). To prevent side-light entering below the crowns at low solar angles, we assumed that there was an opaque forest surrounding the mapped area, to the mean tree height at that site. The total leaf area of each crown (L) was estimated from an allometric regression between leaf mass and diameter at breast height (D) (Keith et al. 2000) and the crown average specific leaf area (4.85 m^2 kg^{-1}) as:

$$L = 4.85 e^{3.625 + 1.575 \ln D} \quad (3)$$

According to Keith et al. (2000), this allometric relationship was estimated from unpublished data of Raison et al. and had an r^2 of 0.919 (n = 11 trees). The trees measured by Raison et al. were comparable to those measured here, being 25 to 86 years old and having a DBH in the range 11.9–83.2 cm, but were harvested in the Brindabella Ranges, ACT.

Foliage was assumed to be evenly distributed within the crown. Mean leaf incidence angle was estimated to be 77° from hemispherical photographs. Meteorological data (incident radiation, air temperature and relative humidity) on a 15-min time step were obtained from the Tumbarumba flux tower (Figure 1; Leuning et al. 2005). Photosynthesis and transpiration routines were parameterized from the leaf-level gas exchange measurements.

We tested the model's simulation of several different features of the sap flow data, including: peak transpiration rates for different trees; total daytime transpiration; responses to environmental variables; and diurnal patterns of water use. Simulation outputs were compared with measured data based on r^2 and model efficiency (ME) statistics (Mayer and Butler 1993).

Results

Leaf gas exchange

Typical daily patterns of spot measurements of g_s are shown in Figure 3. For all trees, g_s increased rapidly between 0730 and 1030 h, and decreased rapidly between 1600 and 1630 h, coinciding with the times that sunlight reached the canopy. However, the time of peak g_s varied according to leaf aspect. Peak g_s was observed midmorning in east-facing leaves (Tree 2) and mid-afternoon in west-facing leaves (Tree 6). Incident PAR was thus a strong driver of g_s.

The Ball-Berry model (Equation 1) was fitted to the combined dataset from all trees. Fitted parameters are given in Table 2. We used regression analysis (Kleinbaum et al. 1998,

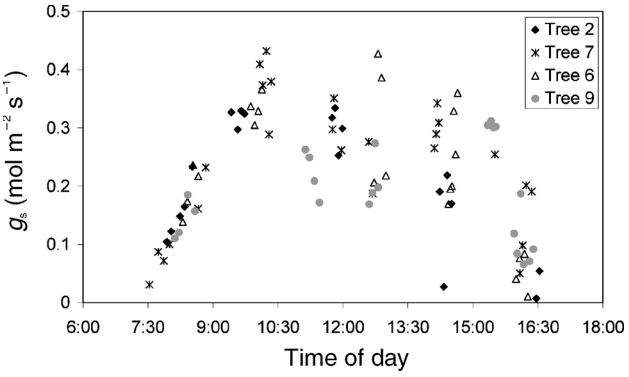

Figure 3. Typical daily patterns of leaf stomatal conductance (g_s) in four of the measured trees. Each measurement was made on a different leaf.

p 327) to test if the slope of the equation (g_1) was similar for all sub-sites, and found that it was significantly less ($P < 0.05$) at Sub-site 5 than at the other sub-sites. It did not differ significantly between the two measurement trees at Sub-site 5. Separate parameters for Sub-sites 1–4 and Sub-site 5 are given in Table 2.

We examined residuals of the g_s model to determine if there was any systematic bias. For trees at Sub-sites 1–4, the residuals were correlated with time of measurement, with the model underpredicting measurements in midmorning (particularly between 0830 and 1130 h) and overpredicting in the afternoon (Figure 4a). The distribution of residuals was different for the trees at Site 5, with the model tending to underpredict measured values in the afternoon (Figure 4b).

Close examination of the residuals also showed that g_s did not conform to the model during the morning period of stomatal opening. This period appeared to last for about 30 minutes, and during this time, the model consistently overpredicted g_s (Figure 4a).

Detailed A–C_i and A–PAR curves were measured on 15 leaves sampled from each of the 10 trees. Photosynthetic parameters were fitted to data from each leaf. Means and standard deviations of each parameter are given in Table 3. Because these parameters were poorly correlated with leaf nitrogen, phosphorus and chlorophyll and specific leaf area, it was assumed that mean parameter values could be used to parameterize the canopy.

We tested how well the combined leaf photosynthesis–stomatal conductance model could predict measured values by comparing g_s predicted by the combined model with the

Table 2. Parameters fitted to the Ball-Berry Equation 1 from stomatal conductance data. Standard errors are given in brackets.

Dataset	g_0 (mol m^{-2} s^{-1})	g_1 (dimensionless)	r^2	n
All data	0.051 (0.009)	11.1 (0.53)	0.703	185
Sub-sites 1–4	0.054 (0.010)	11.6 (0.60)	0.729	142
Sub-site 5	0.036 (0.016)	9.82 (0.95)	0.722	43

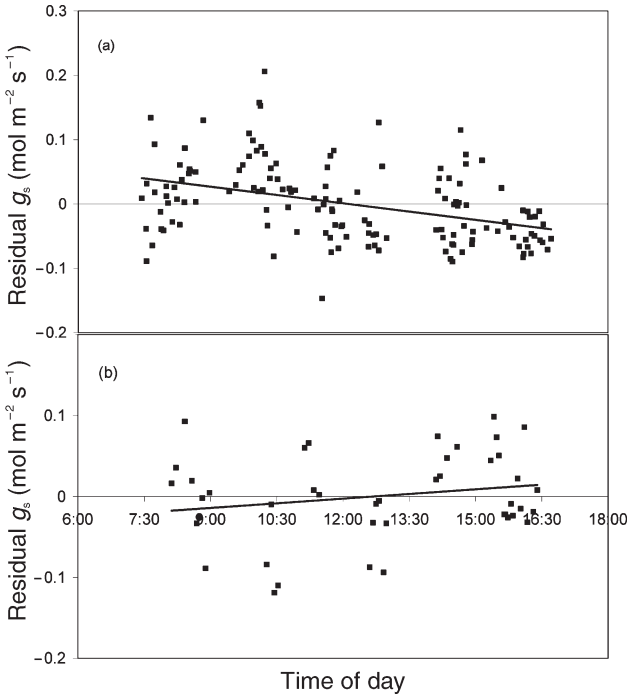

Figure 4. Residuals of leaf stomatal model compared with time of day for (a) Sites 1–4 and (b) Site 5. The residuals are expressed as measured g_s – modeled g_s, where g_s is stomatal conductance. Trend-lines fitted to residuals have r^2 values of (a) 0.16 and (b) 0.04.

spot measurements (Figure 5). As expected, use of the combined photosynthesis–stomatal conductance model resulted in reduced model efficiency compared with the stomatal model alone, but the fit to data was still reasonable (ME = 0.49). For trees 1–4, residuals remained correlated with time of day, as for the stomatal model alone (data not shown).

Tree water use

Modeled tree transpiration is compared with measured sap flow in Figure 6. Regression coefficients for the comparison are given in Table 4. Overall, the model reproduces much of the variation in sap flow among trees and over time. However, there are some discrepancies, which provide insight into errors in our scaling scheme.

Maximum daily rates of tree water use are predicted reason-

Table 3. Photosynthetic parameters estimated from A–C_i and A–PAR curves. Mean and standard deviation across 15 leaves. Abbreviations: J_{max25}, potential rate of electron transport at 25 °C; V_{cmax25}, maximum rate of carboxylation by Rubisco at 25 °C; R_{d25}, leaf dark respiration rate at 25 °C; and α_J, quantum yield of electron transport.

Parameter	Mean	Standard deviation
J_{max25} (μmol m^{-2} s^{-1})	194.6	23.3
V_{cmax25} (μmol m^{-2} s^{-1})	81.5	13.8
R_{d25} (μmol m^{-2} s^{-1})	2.55	0.67
α_J (mol mol^{-1})	0.26	0.03

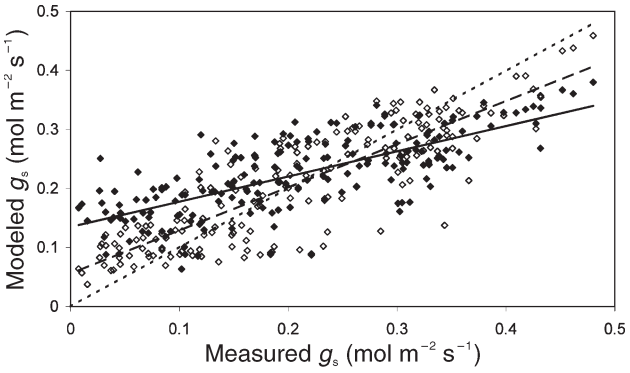

Figure 5. Modeled versus measured leaf stomatal conductance (g_s). Dotted line shows the 1:1 line. Open symbols and dashed line show the predictions of the stomatal model alone (ME = 0.73) and closed symbols and solid line show the predictions of the coupled A–g_s model (ME = 0.49).

ably well, but are higher than measured for some trees and lower than measured for others (Figure 7). This difference among trees occurs because modeled tree water use is strongly related to leaf area, whereas measured sap flow per unit leaf area is more variable among trees. Tree leaf area was estimated from DBH based on an allometric equation, so it is possible that our leaf area estimates are inaccurate. We also investigated whether there were differences in nutrition among trees that could have caused g_s and assimilation rates to vary among trees. There were some differences in mean leaf nitrogen concentration among trees, but these tended to vary by site (Sites 1 and 5 having the highest leaf nitrogen). In general, the model overestimated sap flow in one of two trees at each site, suggesting that nutrition does not explain the discrepancies in maximum tree water use. Inaccuracies in our estimates of leaf area are more likely.

Measured sap flow was lower in the final 2 days of the week, consistent with the lower VPD and PAR on these days (Figure 1). The model captured this difference among days reasonably well (Figure 6), although daytime totals of transpiration suggest that the model is overly sensitive to the low incident PAR and VPD on Day 4 (Table 5). Modeled daytime transpiration, averaged across all trees, is lower than measured on Day 4, whereas it is equal to or higher than measured on the other days. Response surfaces of modeled:measured transpiration also indicate that the model is overly sensitive to incident PAR and VPD. A plot of the ratio of modeled transpiration:measured sap flow against incident PAR for low-VPD and high-VPD conditions shows that the ratio is lowest at low PAR and low VPD (Figure 8).

Diurnal time-courses of sap flow and modeled transpiration, averaged over the five measurement days, are shown in Figure 9. The time-courses are normalized to facilitate comparison of diurnal patterns. The timing of maximum sap flow corresponds well with the timing of maximum transpiration for most trees, with the exception of Trees 6, 9 and 10. Trees 9 and 10 are smaller trees and shaded by a larger dominant tree. Modeled transpiration responds to the shadow cast by the larger tree, with clear sunlit and shaded periods evident in the diurnal time course. The sap flow pattern did not show these fluctuations, likely because sap flow is buffered by water storage in the stem. Because of this buffering effect, we would expect the general pattern of sap flow to correspond to that of predicted transpiration, but not to show rapid changes. The lack of correspondence between diurnal time-courses of sap flow and transpiration for Tree 6 is more puzzling. Transpiration is predicted to peak in the afternoon for this tree, because of its westward facing exposure, similar to Tree 5 at the same site. Leaf-level measurements showed that stomatal conductance peaked in the early afternoon for Tree 6 (Figure 3). It is unclear why sap flow peaked earlier than predicted for this tree but not for others.

The model's ability to predict the start and finish times of

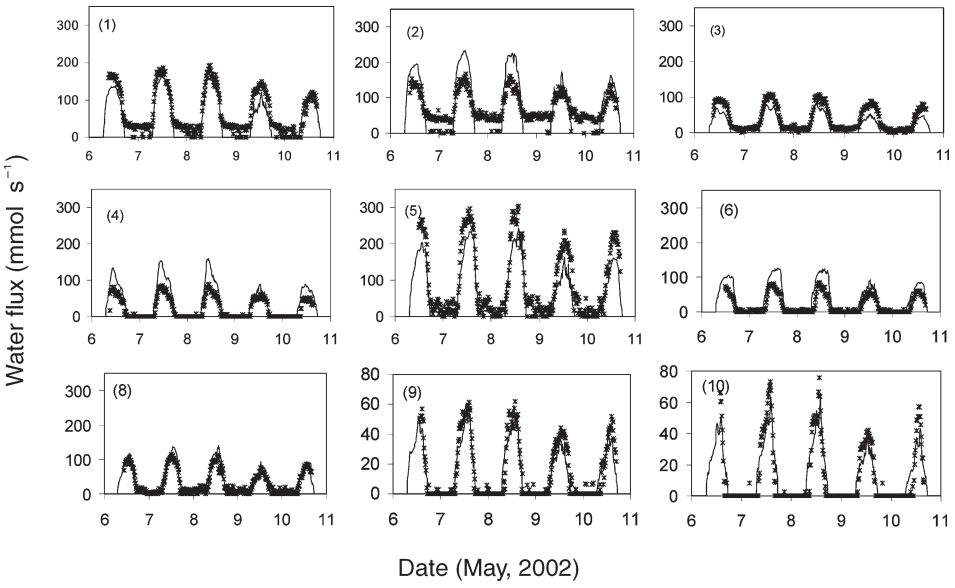

Figure 6. Comparison of modeled transpiration with sap flow data for each measured tree (1–10). Crosses are measured sap flow, and lines are MAESTRA output. Note change of scale for Trees 9 and 10. Statistics for correlations of modeled transpiration versus sap flow are given in Table 4.

Table 4. Statistics for comparison of modeled transpiration (y) against measured sap flow (x) for each tree. Root mean square error (RMSE) is in mmol tree^{-1} s^{-1}.

Tree	Equation	RMSE	r^2
1	$y = 0.82x + 0.44$	28.2	0.81
2	$y = 1.6x - 28.7$	48.2	0.78
3	$y = 0.6x + 4.1$	27.4	0.73
4	$y = 1.40x + 14.8$	38.2	0.81
5	$y = 0.73x + 5.3$	54.0	0.85
6	$y = 1.16x + 28$	38.4	0.76
8	$y = 1.03x + 6.5$	17.0	0.81
9	$y = 0.66x + 8.1$	9.6	0.73
10	$y = 0.56x + 12.7$	11.5	0.80

sap flow is affected by water storage in the stem. Other studies have shown that sap flow measured at breast height lags canopy transpiration by 0–3 hours (Phillips et al. 1997) because of stem capacitance. Comparison of modeled transpiration and measured sap flow in this study (Figure 9) indicates a short lag of about 15–30 min in most trees. The explanatory power, or r^2, of the model increased for Trees 3, 4 and 9 when modeled values were lagged by 15–30 min (data not shown). This increase was most dramatic for Tree 3, where r^2 increased from 0.73 to 0.81 when a lag of 30 min was used.

Although there was a pattern in the residual of g_s over the course of the day (Figure 4), there was no corresponding pattern in the tree water use residuals. Based on the pattern shown in Figure 4, it might be expected that the model would tend to underestimate midmorning sap flow and overestimate midafternoon sap flow. No such pattern was evident. Model error in estimating the canopy radiation environment appears to overwhelm this relatively small leaf-scale error.

We assumed that g_s was zero in the dark, and hence, transpiration was predicted to be zero at nighttime. However, Trees 1, 2, 3 and 5 showed significant sap flow at nighttime (Figure 6). We consider the implications of this finding below.

The model thus appears to capture much of the variation in sap flow for most measured trees. To specifically test whether

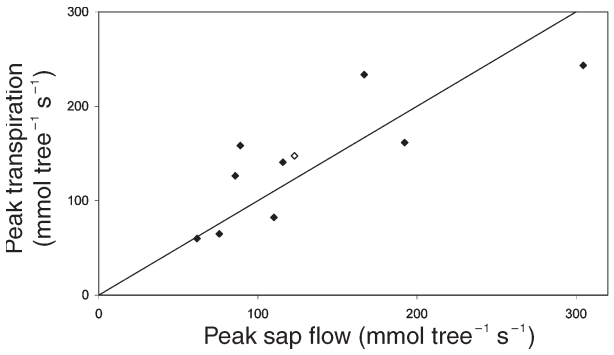

Figure 7. Maximum modeled transpiration over the week plotted against maximum sap flow. Filled symbols give data for each measurement tree; open symbol indicates the mean of all nine trees.

Table 5. Daytime totals of tree transpiration, averaged across all measurement trees. Values are given in mol tree^{-1} day^{-1}. Note that May 6 and May 10 were partial days.

Date	Measured sap flow	Modeled transpiration	Ratio
May 6	2.12	2.15	1.01
May 7	3.27	3.54	1.08
May 8	3.05	3.45	1.13
May 9	2.48	2.04	0.82
May 10	1.91	2.04	1.07

the model was capturing variation among the trees, we calculated r^2 values for each model output against each tree, thus testing whether each tree could have been better modeled by the set of parameters obtained for a different tree. These values are given in Table 6 and show that, in most cases, the specified model for a given tree is close to the best model for that tree. Tree 6 is fairly poorly modeled, as mentioned previously. Tree 9 is better fitted by models for several other trees, largely because, for that tree, the model simulates swift responses to short periods of shade that do not appear in the sap flow data (cf. Figure 9).

We also investigated whether using different stomatal conductance parameters for Trees 9 and 10 (cf. Table 2) improved the model fit for these data by simulating sap flow for these trees based on the parameters for Trees 1–8 (Figure 10). Changing these parameters changes the overall magnitude of predicted sap flow, but does not change the pattern. Hence, r^2 values were little affected by the choice of parameters, suggesting r^2 values will be improved only by incorporating additional second-order effects into the model. Model efficiency was marginally reduced by the use of parameters for all trees, from 0.88 to 0.87 for Tree 9 and from 0.85 to 0.81 for Tree 10. Given that the magnitude of sap flow is uncertain because of the uncertainty in leaf area, it is difficult to say which of the two parameterizations performs better for these trees.

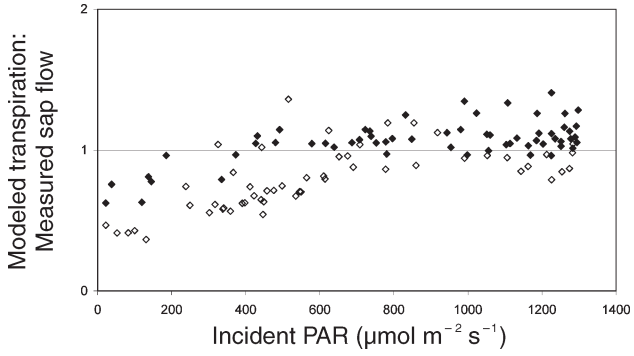

Figure 8. The ratio of modeled transpiration to measured sap flow as a function of incident photosynthetically active radiation (PAR). Filled symbols show data at high vapor pressure deficit (VPD > 0.9 kPa) and open symbols show data at low VPD (< 0.68 kPa). Values are for Tree 2 (values for other trees were similar). Modeled and measured values were normalized by their respective peak values before the ratio was taken.

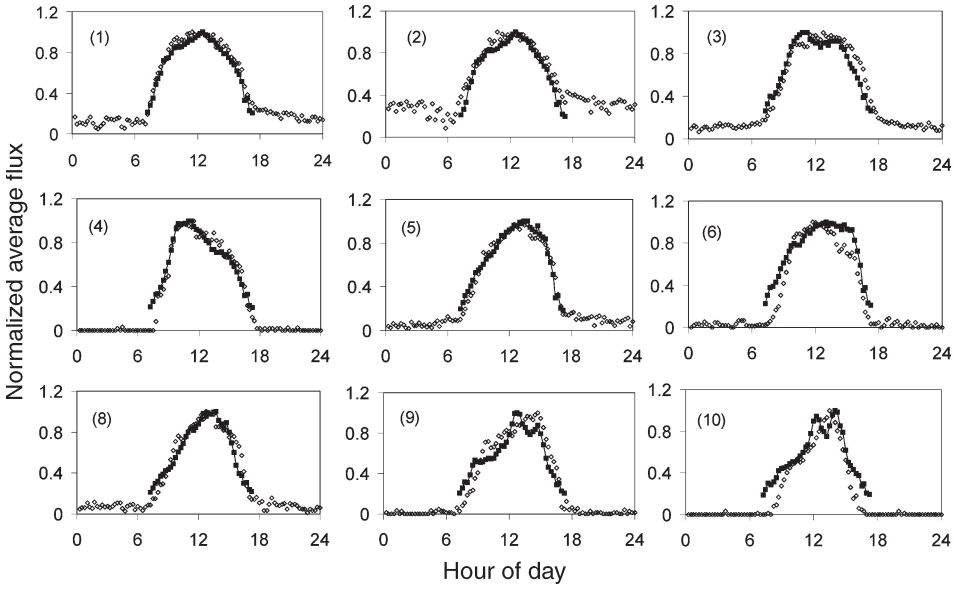

Figure 9. Mean diurnal courses of measured sap flow (open symbols) and modeled transpiration (closed symbols and line). Both datasets were normalized to their maximum value before averaging over the five measurement days, to allow easy comparison of the diurnal pattern.

Discussion

Our main objective was to examine the ability of a model to scale from leaf-level to canopy-level processes. We achieved this objective by using an individual-tree based model applied to simultaneous measurements of leaf and canopy transpiration, allowing a direct test of the ability of the model to scale between these levels. Previous attempts to evaluate canopy models have had to parameterize additional processes. For example, comparisons of canopy models against eddy flux data or canopy chamber data must account for soil fluxes and plant respiration (e.g., Amthor et al. 1994, Van Wijk et al. 2000, Kramer et al. 2002, Medlyn et al. 2005*b*). Similarly, comparisons of one-dimensional canopy models against sap flow data must scale from tree sap flow to whole-canopy transpiration (e.g., Williams et al. 2001). In contrast, the exercise carried out here allows a direct evaluation of model scaling from leaf to crown.

We compared modeled estimates of individual tree transpiration against estimates of tree water use based on sap flow measurements. In assessing this comparison, we also considered several errors associated with implementation of the sap flow technique itself. The sap flow estimates are sensitive to the assumed wound size, which we assumed to be 3.1 mm (O'Grady 2000). However, wound development takes 5–7 days, so wound size would have changed during the measurement campaign. This change over time would mean that sap velocity is slightly overestimated, but this effect would be consistent across the trees. An important error that could vary on a tree by tree basis is associated with estimating sapwood area, because scaling from sap velocity to total tree water flux is highly sensitive to errors in the estimation of sapwood area. We used cores from the measurement trees to estimate sapwood area and confirmed these values based on a calibration between diameter and sapwood area measured on felled trees. Another important source of error could arise from probe misalignment. This source of error, which is difficult to resolve using the compensation heat pulse technique, may lead to an overestimate of sap velocity, particularly at low velocities. We used a drilling rig to minimize problems with probe alignment. The overall error in the sap-flow-based estimates of tree water

Table 6. Matrix of r^2 values for model output for each tree (Model 1–10) compared to sap flow data for each tree (Tree 1–10). Bold values indicate the r^2 of the model when parameterized for that tree; underlined values indicate where the model has a higher r^2 when parameterized for a different tree (i.e., highest values in a given column).

	Tree 1	Tree 2	Tree 3	Tree 4	Tree 5	Tree 6	Tree 8	Tree 9	Tree 10
Model 1	**0.796**	0.782	0.645	0.774	0.755	0.743	0.782	0.649	0.627
Model 2	0.775	**0.774**	0.622	0.746	0.741	0.724	0.765	0.638	0.648
Model 3	0.792	0.778	**0.726**	0.818	0.783	0.797	0.797	0.722	0.673
Model 4	0.735	0.723	0.595	**0.808**	0.657	0.759	0.696	0.553	0.504
Model 5	0.676	0.674	0.722	0.646	**0.846**	0.730	0.862	0.805	0.704
Model 6	0.722	0.688	0.760	0.698	0.860	**0.753**	0.875	0.814	0.657
Model 8	0.624	0.667	0.683	0.602	0.796	0.714	**0.811**	0.762	0.794
Model 9	0.647	0.646	0.661	0.558	0.762	0.634	0.768	**0.745**	0.768
Model 10	0.580	0.608	0.641	0.515	0.706	0.603	0.701	0.715	**0.800**

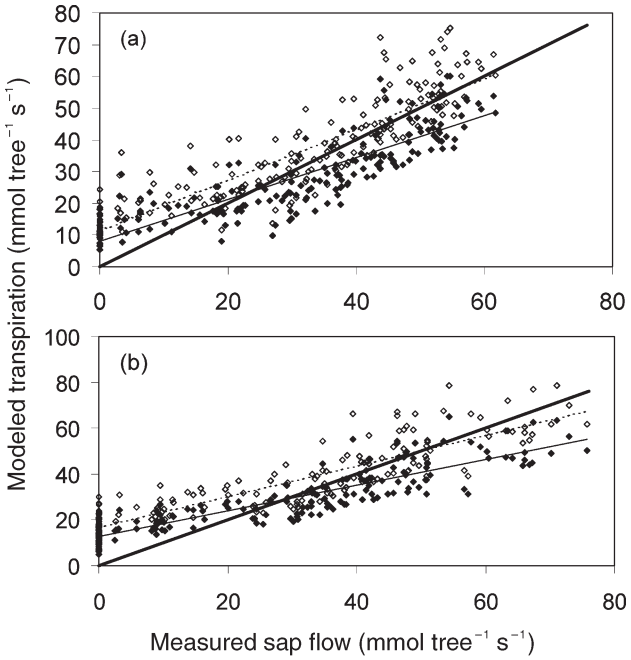

Figure 10. Comparison of modeled transpiration against measured sap flow for Trees 9 and 10. Filled symbols and solid line, simulations with parameters for Trees 9 and 10; open symbols and dashed line, simulations with parameters for all trees; bold line, 1:1 line. The regression fits were as follows: For Tree 9 with parameters for Trees 9 and 10, $y = 0.66x + 8.1$, $r^2 = 0.73$, ME = 0.88; with parameters for all trees, $y = 0.8x + 11.4$, $r^2 = 0.74$, ME = 0.87. For Tree 10 with parameters for Trees 9 and 10, $y = 0.67x + 16.9$, $r^2 = 0.80$, ME = 0.85; with parameters for all trees, $y = 0.56x + 12.7$, $r^2 = 0.80$, ME = 0.81.

use is likely to be of the order of 10% when sap velocity is high (Hatton et al. 1995, Vertessey et al. 1997).

We tested the ability of the model to simulate several features of the sap flow data, including peak transpiration, mean daily transpiration, response to environmental variables and diurnal patterns of transpiration. The peak transpiration rate was overestimated for some trees and underestimated for others, with errors ranging from –35% to +65% (Figure 7). We detected no pattern in this error, with underestimation and overestimation occurring in neighboring trees, suggesting that the error is not caused by model bias. It seems more likely that it is a result of error in tree leaf area estimation. Leaf area was estimated based on an allometric regression for leaf mass against DBH, and a mean value for specific leaf area (SLA). The error for the allometric regression was low (mean square error = 0.4025 kg; Keith et al. 2000), but there will be additional errors in applying the regression to a new site. To estimate the error in leaf area at this site, we used crown size as a proxy for leaf area. A regression of crown size against DBH had an r^2 of 0.76 but crown size of individual trees differed from predicted values by –50% to +40%, similar to the range in error in peak transpiration rate. This error is likely to be reduced in stand-scale simulations because estimates of stand leaf area are more accurate than those for individual trees. For example, the error in daily transpiration, when averaged across all nine measurement trees, was considerably lower than the error for individual tree transpiration (Table 5).

Another potential source of error in estimating peak transpiration rates is our use of leaf-level measurements made at the base of the canopy to represent leaf processes throughout the canopy. Because the cherry-picker reached only to 20 m, we could reach only the lower third of most tree crowns. The exception was the smaller trees measured at Sub-site 5, where we sampled the top of the tree crown. Our experimental design raises two questions: (1) how representative of the average leaf are the measurement leaves; and (2) what bias is introduced by using mean parameters rather than a distribution (e.g., Rastetter et al. 1992)? Most forest canopies show a gradient in leaf properties with increasing depth (e.g., Meir et al. 2002), suggesting that leaves at the base of the canopy are unlikely to be representative. We found a gradient in leaf nitrogen on an area basis, with mean values ranging from 2.5 g m^{-2} in the lower third of the canopy to 3.0 g m^{-2} in the upper third. This gradient was mainly driven by differences in specific leaf area. However, variability around these mean values was high, and the leaves sampled at the canopy base had nitrogen concentrations ranging from 2 to 3.5 g m^{-2}, indicating that we sampled across the full range of leaf nitrogen concentrations. These are open canopies, with pendulous leaves and a low leaf area index, so the gradient between canopy top and base is less than in other forest types. Another unusual feature of this forest type is that there is a poor relationship between leaf nutrition and gas exchange properties. Although strong relationships between conductance, photosynthesis and leaf nitrogen are found for many tree species (e.g., Schulze et al. 1994, Medlyn et al. 1999), *Eucalyptus* leaves commonly do not show these relationships (e.g., Leuning et al. 1991, Close et al. 2004). We found no significant correlation between leaf gas exchange and leaf nutrition. Thus, for this forest type, the use of mean leaf parameters, rather than a parameter distribution, is unlikely to introduce bias in the estimates of peak transpiration.

A comparison of the temporal variability of sap flow with modeled transpiration is of interest, because our model is able to reproduce the radiation environment of individual tree crowns. Most of the measurement trees were smaller and shorter than average trees, allowing us to test the ability of the model to simulate shading by surrounding tree crowns. For most trees, the model captured the diurnal pattern of sap flow well, with some buffering evident (Figure 9), showing that differences in time-courses of sap flow among trees can be explained by differences in their local radiation environment. There was a short time lag between modeled transpiration and sap flow data, of the order of 15–30 min. This lag is less than that found for conifers and rain forest trees (Phillips et al. 1997). Although these trees are tall, ranging in height from 20 to 40 m, they have a high hydraulic conductance (Mokany et al. 2003) such that sap flow responds rapidly to transpirational demand.

It is informative to contrast the performance of the leaf and canopy scale models. Based on the residuals of the g_s model, we anticipated that the model might underestimate transpiration around mid-morning and overestimate it in midafternoon.

This pattern is consistent with other g_s data that tend to show a depression after midday, which may be related to reduced water supply as soil dries around fine roots (e.g., Tognetti et al. 1998, Brodribb and Holbrook 2004). However, when scaling to the canopy, this morning–afternoon trend in residuals is not seen, perhaps because this source of error is overwhelmed by the error in estimating the radiation environment of the canopy. Alternatively, there may be some compensation at the canopy scale unaccounted for in the model.

A second area of difference between leaf and canopy scale models is the sensitivity to environmental conditions. Figure 8 illustrates that the canopy-scale model is overly sensitive to incident PAR at low VPD, simulating a stronger reduction in transpiration than observed on a cloudy humid day. The leaf-scale model, in contrast, is less sensitive to environmental conditions than the measurements (Figure 5). This contrast between models seems to indicate that leaf conductance is more sensitive to PAR than canopy conductance. Various hypotheses could explain such a difference in behavior at different scales. For example: if an individual leaf is shaded, it may be optimal for stomata on that leaf to shut, saving water for use by sunlit leaves elsewhere in the canopy; whereas if the entire canopy receives low light on an overcast day, stomata throughout the canopy may remain open to maximize photosynthesis. This difference in behavior at different scales warrants further research.

Overall, the discrepancies between modeled and measured tree transpiration are relatively minor. Although the model performed well during the measurement week, we asked how well it might perform during the rest of the year. In particular, g_s and transpiration of eucalypts are reduced during drought (e.g., Crombie 1992, David et al. 1997, Prior et al. 1997, Mielke et al. 2000). Soil water content during this campaign was 0.27 cm^3 cm^{-3}. Stomatal conductance measurements were also made in the canopy in November 2001 and March 2005 when the soil water content was 0.33 and 0.29 cm^3 cm^{-3}, respectively. The stomatal model (Equation 1) was fitted to these datasets, and identical parameter values were obtained, indicating that these parameters are valid for periods with soil water content > 0.27 cm^3 cm^{-3}. During the period July 2001–May 2005, the soil water content remained above this value except for two periods of severe drought, from November 2002 to April 2003 and February 2004 to April 2004 (Leuning et al. 2005). These results indicate that the model should be applicable except during severe droughts.

The sap flow data indicated significant flows at nighttime in several trees. It is possible that these data are in error. The compensation heat-pulse technique is subject to error in resolving low flows. However, nighttime sap flow has been confirmed in several studies (Benyon 1999, Snyder et al. 2003, Bucci et al. 2004, Daley and Phillips 2006). These flows have been attributed to stem refilling (Phillips et al. 2003) or to stomata remaining open at night (Snyder et al. 2003) and are often correlated with wind speed and vapor pressure deficit (Daley and Phillips 2006). Our measurements indicate that stomata shut at the end of the day in all measured trees, to the limit of resolution of the gas exchange measurements. If the nighttime sap flow was due to stem refilling, it might be expected that daytime sap flow would be less than predicted, because of the use of stored water. However, this was the case only for Tree 2; for Trees 1, 3 and 5, not only was there nighttime sap flow, but daytime sap flow exceeded that predicted. The significance of the observed nighttime sap flow remains to be resolved, but eddy covariance measurements at this site suggest that nighttime stand water use is minimal (Helen Cleugh, CSIRO Marine and Atmospheric Research, Canberra, Australia, personal communication).

Variability among trees also appears to be well captured, with the model generally performing best when parameterized for the measured tree (Table 6). The g_s data indicate that there were differences in stomatal behavior among the trees, with Trees 9 and 10 having the lowest conductances. We hypothesize that the water relations of these trees were relatively poor because they were smallish trees growing beneath an overarching large tree that may have been out-competing them for water. It is possible that competition among trees in these open eucalypt forests is for water rather than for light. However, because of the uncertain leaf area of the trees, we were unable to confirm whether this reduced leaf-level stomatal conductance was manifested in lower whole-tree transpiration. A better understanding of how and why the stomatal conductance relationship varies among trees is needed.

Conclusions

We tested the ability to scale from leaf-level to tree-level processes with an individual-tree model and datasets that were measured simultaneously at the leaf and tree scales. Some discrepancies between data and model output were found, highlighting areas where our understanding is poor. Our study raised several questions. For example, why is the canopy-scale model more sensitive to environmental conditions than measurements, whereas the leaf-scale model is less sensitive than measurements? How do leaf conductance parameters vary among trees, and how does the variation depend on tree water relations?

Overall, however, the model performed well. Errors in estimating peak transpiration were likely caused by errors in estimating leaf area for individual trees and became much smaller when averaged over several trees. The model also simulated the time-course of transpiration well. Although the study was carried out with an individual-tree based model, it has implications for the more widely used one-dimensional canopy models, because the structure, assumptions and performance of the different types of models are comparable (Hanson et al. 2004). A recent model evaluation (Abramowitz et al. 2007) indicated that total latent heat flux estimated by land surface schemes is biased. Our study suggests that the canopy component of latent heat flux estimated by land surface models is unlikely to be biased and that efforts should be concentrated on improving estimates of soil and understory components of the flux.

Acknowledgments

We thank John Smith for technical assistance. Ray Leuning and Steve Zegelin provided the site meteorological and soil water data. CSIRO Climate Program provided access to the Tumbarumba OzFlux site and use of the cherry picker truck. We thank Ross McMurtrie for helpful discussions. Ying-Ping Wang provided the original code for the MAESTRO model. BM was supported by an ARC Post-Doctoral Fellowship. DAP and APO thank the Australian Research Council for financial support.

References

Abramowitz, G., A. Pitman, H. Gupta, E. Kowalczyk and Y.P. Wang. 2007. On the need for a biophysically based benchmark for land surface models. J. Hydrometeorol. In press.

Amthor, J.S., M.L. Goulden, J. Munger and S. Wofsy. 1994. Testing a mechanistic model of forest-canopy mass and energy exchange using eddy correlation: carbon dioxide and ozone uptake by a mixed oak–maple stand. Aust. J. Plant Physiol. 21:623–651.

Ball, J.T., I.E. Woodrow and J.A. Berry. 1987. A model predicting stomatal conductance and its contribution to the control of photosynthesis under different environmental conditions. *In* Progress in Photosynthesis Research. Ed. J. Biggins. Martinus-Nijhoff Publishers, Dordrecht, The Netherlands, pp 221–224.

Benyon, R.G. 1999. Nighttime water use in an irrigated *Eucalyptus grandis* plantation. Tree Physiol. 19:853–859.

Bernacchi, C.J., E.L. Singsaas, C. Pimentel, A.R. Portis and S.P. Long. 2001. Improved temperature response functions for models of Rubisco-limited photosynthesis. Plant Cell Environ. 24:253–259.

Brodribb, T.J. and N.M. Holbrook. 2004. Diurnal depression of leaf hydraulic conductance in a tropical tree species. Plant Cell Environ. 27:820–827.

Bucci, S.J., F.G. Scholz, G. Goldstein, F.C. Meinzer, J.A. Hinojosa, W.A. Hoffmann and A.C. Franco. 2004. Processes preventing nocturnal equilibration between leaf and soil water potential in tropical savanna woody species. Tree Physiol. 24:1119–1127.

Close, D.C., M. Battaglia, N.J. Davidson and C.L. Beadle. 2004. Within-canopy gradients of nitrogen and photosynthetic activity of *Eucalyptus nitens* and *Eucalyptus globulus* in response to nitrogen nutrition. Aust. J. Bot. 52:133–140.

Crombie, D.S. 1992. Root depth, leaf-area and daytime water relations of jarrah (*Eucalyptus marginata*) forest overstorey and understorey during summer drought. Aust. J. Bot. 40:113–122.

Daley, M.J. and N.G. Phillips. 2006. Interspecific variation in nighttime transpiration and stomatal conductance in a mixed New England deciduous forest. Tree Physiol. 26:411–419.

David, T.S., M.I. Ferreira, J.S. David and J.S. Pereira. 1997. Transpiration from a mature *Eucalyptus globulus* plantation in Portugal during a spring–summer period of progressively higher water deficit. Oecologia 110:153–159.

Edwards, W.R.N. and N.W.M. Warwick. 1984. Transpiration from a kiwifruit vine as estimated by the heat pulse technique and the Penman-Monteith equation. N.Z. J. Agric. Res. 27:537–543.

Farquhar, G.D., S. von Caemmerer and J.A. Berry. 1980. A biochemical model of photosynthetic carbon dioxide assimilation in leaves of 3-carbon pathway species. Planta 149:78–90.

Gedney, N., P.M. Cox, R.A. Betts, O. Boucher, C. Huntingford and P.A. Stott. 2006. Detection of a direct carbon dioxide effect in continental river runoff records. Nature 439:835–838.

Gordon, W.S. and J.S. Famiglietti. 2004. Response of the water balance to climate change in the United States over the 20th and 21st centuries: results from the VEMAP Phase 2 model intercomparisons. Global Biogeochem. Cycles 18: doi:1029/2003 GB002098.

Hanson, P.J., J.S. Amthor, S.D. Wullschleger et al. 2004. Oak forest carbon and water simulations: model intercomparisons and evaluations against independent data. Ecol. Monogr. 74:443–489.

Hatton, T.J., E.A. Catchpole and R.A. Vertessy. 1990. Integration of sapflow velocity to estimate plant water-use. Tree Physiol. 6:201–209.

Hatton, T.J., J. Walker, W.R. Dawes and F.X. Dunin. 1992. Simulations of hydroecological responses to elevated CO_2 at the catchment scale. Aust. J. Bot. 40:679–696.

Hatton, T.J., S.J. Moore and P.H. Reece. 1995. Estimating stand transpiration in a *Eucalyptus populnea* woodland with the heat pulse method—measurement errors and sampling strategies. Tree Physiol. 15:219–227.

Jarvis, P.G. 1976. The interpretation of the variations in leaf water potential and stomatal conductance found in canopies in the field. Phil. Trans. Roy. Soc. Lond. B 273:593–610.

Jarvis, P.G. 1995. Scaling processes and problems. Plant Cell Environ. 18:1079–1089.

Jones, H.G. 1992. Plants and Microclimate, 2nd Edn. Cambridge University Press, Cambridge, 428 p.

Keith, H., D. Barrett and R. Keenan. 2000. Review of allometric relationship for estimating woody biomass for New South Wales, the Australian Capital Territory, Victoria, Tasmania and South Australia. National Carbon Accounting System. Tech. Rep. No. 5b. Australian Greenhouse Office, Canberra, 11 p.

Kirschbaum, M.U.F. and G.D. Farquhar. 1984. Temperature-dependence of whole-leaf photosynthesis in *Eucalyptus pauciflora* Sieb ex Spreng. Aust. J. Plant Physiol. 11:519–538.

Kleinbaum, D.G., L.L. Kupper, K.E. Muller and A. Nizam. 1998. Applied regression analysis and other multivariable methods. Duxbury Press, Pacific Grove, CA, 798 p.

Köstner, B., E.M. Falge, M. Alsheimer, R. Geyer and J.D. Tenhunen. 1998. Estimating tree canopy water use via xylem sapflow in an old Norway spruce forest and a comparison with simulation-based canopy transpiration estimates. Ann. Sci. For. 55:125–139.

Kramer, K., I. Leinonen, H.H. Bartelink et al. 2002. Evaluation of six process-based forest growth models using eddy-covariance measurements of CO_2 and H_2O fluxes at six forest sites in Europe. Global Change Biol. 8:213–230.

Lasch, P., F.W. Badeck, F. Suckow, M. Lindner and P. Mohr. 2005. Model-based analysis of management alternatives at stand and regional level in Brandenburg (Germany). For. Ecol. Manage. 207:59–74.

Leuning, R. 1995. A critical appraisal of a coupled stomatal–photosynthesis model for C_3 plants. Plant Cell Environ. 18:339–357.

Leuning, R., Y.P. Wang and R.N. Cromer. 1991. Model simulations of spatial distributions and daily totals of photosynthesis in *Eucalyptus grandis* canopies. Oecologia 88:494–503.

Leuning, R., F.M. Kelliher, D.G.G. Depury and E.D. Schulze. 1995. Leaf nitrogen, photosynthesis, conductance and transpiration—scaling from leaves to canopies. Plant Cell Environ. 18: 1183–1200.

Leuning, R., H.A. Cleugh, S.J. Zegelin and D. Hughes. 2005. Carbon and water fluxes over a temperate Eucalyptus forest and a tropical wet/dry savanna in Australia: measurements and comparison with MODIS remote sensing estimates. Agric. For. Meteorol. 129:151–173.

Mayer, D.G. and D.G. Butler. 1993. Statistical validation. Ecol. Model. 68:21–32.

Medlyn, B.E. 2004. A MAESTRO retrospective. *In* Forests at the Land–Atmosphere Interface. Eds. M. Mencuccini, J. Grace, J.B. Moncrieff and K. McNaughton. CAB International, Wallingford, U.K., pp 105–121.

Medlyn, B.E., F.-W. Badeck, D.G.G. de Pury et al. 1999. Effects of elevated [CO_2] on photosynthesis in European forest species: a meta-analysis of model parameters. Plant Cell Environ. 22:1475–1495.

Medlyn, B.E., E. Dreyer, D. Ellsworth et al. 2002. Temperature response of parameters of a biochemically-based model of photosynthesis. II. A review of experimental data. Plant Cell Environ. 25:1167–1179.

Medlyn, B.E., D.J. Barrett, J.J. Landsberg, P. Sands and R. Clement. 2003. Conversion of canopy intercepted radiation to photosynthate: modeling approaches at regional scales. Funct. Plant Biol. 30:153–169.

Medlyn, B.E., A.P. Robinson, R. Clement and R.E. McMurtrie. 2005*a*. On the validation of models of forest CO_2 exchange using eddy covariance data: some perils and pitfalls. Tree Physiol. 25: 839–857.

Medlyn, B.E., P. Berbigier, R. Clement et al. 2005*b*. Carbon balance of coniferous forests growing in contrasting climates: model-based analysis. Agric. For. Meteorol. 131:97–124.

Meir, P., B. Kruijt, M. Broadmeadow, E. Barbosa, O. Kull, F. Carswell, A. Nobre and P.G. Jarvis. 2002. Acclimation of photosynthetic capacity to irradiance in tree canopies in relation to leaf nitrogen concentration and leaf mass per unit area. Plant Cell Environ. 25:343–357.

Meiresonne, L., D.A. Sampson, A.S. Kowalski, I.A. Janssens, N. Nadezhdina, J. Čermák, J. Van Slycken and R. Ceulemans. 2003. Water flux estimates from a Belgian Scots pine stand: a comparison of different approaches. J. Hydrol. 270:230–252.

Mielke, M.S., M.A. Oliva, N.F. de Barros, R.M. Penchel, C.A. Martinez, S. da Fonseca and A.C. de Almeida. 2000. Leaf gas exchange in a clonal eucalypt plantation as related to soil moisture, leaf water potential and microclimate variables. Trees 14:263–270.

Mokany, K., R.E. McMurtrie, B.J. Atwell and H. Keith. 2003. Interaction between sapwood and foliage area in alpine ash (*Eucalyptus delegatensis*) trees of different heights. Tree Physiol. 23:949–957.

Morales, P., M.T. Sykes, I.C. Prentice et al. 2005. Comparing and evaluating process-based ecosystem model predictions of carbon and water fluxes in major European forest biomes. Global Change Biol. 11:2211–2233.

O'Grady, A.P. 2000. Patterns of tree and stand water use in the eucalypt open forests of northern Australia. Ph.D. Thesis. Northern Territory University, Darwin, Australia, 165 p.

Oreskes, N., K. Schrader-Frechette and K. Belitz. 1994. Verification, validation and confirmation of numerical models in the earth sciences. Science 263:641–645.

Phillips, N., A. Nagchaudhuri, R. Oren and G. Katul. 1997. Time constant for water transport in loblolly pine trees estimated from time series of evaporative demand and stem sapflow. Trees 11:412–419.

Phillips, N.G., M.G. Ryan, B.J. Bond, N.G. McDowell, T.M. Hinckley and J. Čermák. 2003. Reliance on stored water increases with tree size in three species in the Pacific Northwest. Tree Physiol. 23:237–245.

Porra, R.J., W.A. Thompson and P.E. Kriedemann. 1989. Determination of accurate extinction coefficients and simultaneous equations for assaying chlorophyll-a and chlorophyll-b extracted with 4 different solvents—verification of the concentration of chlorophyll standards by atomic absorption spectroscopy. Biochim. Biophys. Acta 975:384–394.

Prior, L.D., D. Eamus and G.A. Duff. 1997. Seasonal and diurnal patterns of carbon assimilation, stomatal conductance and leaf water potential in *Eucalyptus tetrodonta* saplings in a wet-dry savanna in northern Australia. Aust. J. Bot. 45:241–258.

Rastetter, E.B., A.W. King, B.J. Cosby, G.M. Hornberger, R.V. O'Neill and J.E. Hobbie. 1992. Aggregating fine-scale ecological knowledge to model coarser-scale attributes of ecosystems. Ecol. Applic. 2:55–70.

Rayment, G.E. and F.R. Higginson. 1992. Australian laboratory handbook of soil and water chemical methods. Inkata Press, Melbourne, 330 p.

Rykiel, E.J., Jr. 1996. Testing ecological models: the meaning of validation. Ecol. Model. 90:229–244.

Schulze, E.-D., F.M. Kelliher, C. Korner, J. Lloyd and R. Leuning. 1994. Relationships among maximum stomatal conductance, ecosystem surface conductance, carbon assimilation rate and plant nitrogen nutrition—a global ecology scaling exercise. Annu. Rev. Ecol. Syst. 25:629–660.

Silva, M.E.S., S.H. Franchito and V.B. Rao. 2006. Effects of Amazonian deforestation on climate: a numerical experiment with a coupled biosphere–atmosphere model with soil hydrology. Theoret. Appl. Climatol. 85:1–18.

Snyder, K.A., J.H. Richards and L.A. Donovan. 2003. Night-time conductance in C_3 and C_4 species: do plants lose water at night? J. Exp. Bot. 54:861–865.

Swanson, R.H. and D.W.A. Whitfield. 1981. A numerical analysis of heat pulse velocity theory and practice. J. Exp. Bot. 32:221–239.

Tognetti, R., A. Longobucco and A. Raschi. 1998. Vulnerability of xylem to embolism in relation to plant hydraulic resistance in *Quercus pubescens* and *Quercus ilex* co-occurring in a Mediterranean coppice stand in central Italy. New Phytol. 139:437–447.

Vano, J.A., J.A. Foley, C.J. Kucharik and M.T. Coe. 2006. Evaluating the seasonal and interannual variations in water balance in northern Wisconsin using a land surface model. J. Geophys. Res.-Biogeosci. 111: doi: 10.1029/2005JG000112.

Van Wijk, M.T., S.C. Dekker, W. Bouten, F.C. Bosveld, W. Kohsiek, K. Kramer and G.M.J. Mohren. 2000. Modeling daily gas exchange of a Douglas-fir forest: comparison of three stomatal conductance models with and without a soil water stress function. Tree Physiol. 20:115–122.

Vertessy, R.A., T.J. Hatton, P. Reece, S.K. Osullivan and R.G. Benyon. 1997. Estimating stand water use of large mountain ash trees and validation of the sap flow measurement technique. Tree Physiol. 17:747–756.

Walker, G.R., L. Zhang, T.W. Ellis, T.J. Hatton and C. Petheram. 2002. Estimating impacts of changed land use on recharge: review of modeling and other approaches appropriate for management of dryland salinity. Hydrogeol. J. 10:68–90.

Wang, Y.-P. and P.G. Jarvis. 1990. Description and validation of an array model—MAESTRO. Agric. For. Meteorol. 51:257–280.

Wang, Y.-P. and R. Leuning. 1998. A two-leaf model for canopy conductance, photosynthesis and partitioning of available energy. I: model description and comparison with a multi-layered model. Agric. For. Meteorol. 91:89–111.

White, J.D., N.A. Scott, A.I. Hirsch and S.W. Running. 2006. 3-PG productivity modeling of regenerating Amazon forests: Climate sensitivity and comparison with MODIS-derived NPP. Earth Interactions 10:1–26.

Williams, M., B.J. Bond and M.G. Ryan. 2001. Evaluating different soil and plant hydraulic constraints on tree function using a model and sap flow data from ponderosa pine. Plant Cell Environ. 24: 679–690.

Appendix: Calculation of transpiration in MAESTRA

Transpiration is calculated separately for sun and shade foliage at each grid point. The iterative scheme proposed by Wang and Leuning (1998) is used to solve for leaf energy balance. This scheme uses the following steps: (1) assume that leaf surface temperature, VPD and CO_2 concentration (T_s, D_s and C_s) are equal to air temperature, VPD and CO_2 conentration (T_a, D_a and C_a), respectively; (2) calculate leaf photosynthesis and stomatal conductance; (3) calculate boundary layer conductance and radiation conductance; (4) apply Penman-Monteith equation to calculate transpiration; (5) calculate new values for T_s, D_s and C_s.; and (6) if leaf temperature has converged (i.e., is within a given tolerance of previous leaf temperature value), finish: otherwise, return to Step 2.

Boundary layer conductances to heat transfer by free and forced convection and the radiation conductance are calculated according to formulae given by Leuning et al. (1995). The boundary layer conductance for free convection (g_{bHf}, mol m^{-2} s^{-1}) is given by:

$$g_{bHf} = \frac{0.5 D_H (1.6 \times 10^8 |T_s - T_a| w^3)^{0.25}}{w} \left(\frac{P}{RT_k} \right) \quad \text{(A1)}$$

where D_H is molecular diffusivity to heat (21.5 x 10^{-6} m^2 s^{-1}), w is leaf width (here 2 cm), P is atmospheric pressure (Pa), R is the universal gas constant (8.314 J mol^{-1} K^{-1}) and T_k is air temperature in Kelvin. Boundary layer conductance for forced convection (g_{bHu}, mol m^{-2} s^{-1}) is given by:

$$g_{bHu} = 0.003 \sqrt{\frac{U}{w}} \left(\frac{P}{RT_k} \right) \quad \text{(A2)}$$

where U is wind speed (m s^{-1}). The radiation conductance (g_{rN}, mol m^{-2} s^{-1}) is given by:

$$g_{rN} = 4\varepsilon_1 \sigma T_k^4 k_d e^{-k_d \xi} + e^{-k_d (L - \xi)} \quad \text{(A3)}$$

where ε_l is leaf emissivity (0.95), σ is the Stefan-Boltzmann constant (5.67×10^{-8} W m^{-2} K^{-4}), k_d is transmittance of diffuse radiation to the gridpoint, ξ is cumulative leaf area above the gridpoint and L is total leaf area (cf. Wang and Leuning 1998, Table 1, and Jones 1992, p 108).

The Penman-Monteith equation is then calculated according to:

$$\lambda E = \frac{s R_n + D_a g_H c_p M_a}{s + \gamma g_H / g_V} \quad \text{(A4)}$$

where λ is the latent heat of water vapor (J mol^{-1}); E is transpiration per unit leaf area (mol m^{-2} s^{-1}); s is the slope of the curve relating saturation water vapor pressure to temperature (Pa K^{-1}); R_n is isothermal net radiation (W m^{-2}); g_H is total leaf conductance to heat (mol m^{-2} s^{-1}); c_p is the heat capacity of air (1010 J kg^{-1} K^{-1}); M_a is molecular mass of air (29×10^{-3} kg mol^{-1}); γ is the psychometric constant (Pa K^{-1}) and g_V is total leaf conductance to water vapor (mol m^{-2} s^{-1}).

The latent heat of water vapor varies with air temperature according to:

$$\lambda = (2.501 \times 10^6 - 2.365 \times 10^3 T_a)\ 18 \times 10^{-3} \quad \text{(A5)}$$

Isothermal net radiation, R_n, is calculated as the sum of beam, diffuse and scattered radiation absorbed by foliage at the grid-point in three wavebands: PAR, NIR and thermal radiation. The total leaf conductance to heat is given by:

$$g_H = 2(g_{bHf} + g_{bHu} + g_{rN}) \quad \text{(A6)}$$

and total leaf conductance to water vapor, g_v, is calculated as the sum in series of the stomatal conductance and boundary layer conductance. Boundary layer conductance to water vapor is given by:

$$g_{bV} = 1.075 \times 2(g_{bHf} + g_{bHu}) \quad \text{(A7)}$$

where the factor 1.075 accounts for the relative diffusivities of heat and water vapor in air.